

REPORT DOCUMENTATION PAGE

Form Approved
OMB No. 0704-0188

Public reporting burden for this collection of information is estimated to average 1 hour per response, including the time for reviewing instructions, searching existing data sources, gathering and maintaining the data needed, and completing and reviewing this collection of information. Send comments regarding this burden estimate or any other aspect of this collection of information, including suggestions for reducing this burden to Department of Defense, Washington Headquarters Services, Directorate for Information Operations and Reports (0704-0188), 1215 Jefferson Davis Highway, Suite 1204, Arlington, VA 22202-4302. Respondents should be aware that notwithstanding any other provision of law, no person shall be subject to any penalty for failing to comply with a collection of information if it does not display a currently valid OMB control number. PLEASE DO NOT RETURN YOUR FORM TO THE ABOVE ADDRESS.

1. REPORT DATE (DD-MM-YYYY)

30-3-2005

REPRINT

4. TITLE AND SUBTITLE

Monopole-Quadrupole Model of Spacecraft Charging in Sunlight

5a. CONTRACT NUMBER**5b. GRANT NUMBER****5c. PROGRAM ELEMENT NUMBER****6. AUTHOR(S)**

M. Tautz* and S. T. Lai

5d. PROJECT NUMBER

5021

5e. TASK NUMBER

RS

5f. WORK UNIT NUMBER

A1

7. PERFORMING ORGANIZATION NAME(S) AND ADDRESS(ES)

Air Force Research Laboratory/VSBX
29 Randolph Road
Hanscom AFB MA 01731-3010

8. PERFORMING ORGANIZATION REPORT NUMBER

AFRL-VS-HA-TR-2005-1003

9. SPONSORING / MONITORING AGENCY NAME(S) AND ADDRESS(ES)**10. SPONSOR/MONITOR'S ACRONYM(S)**

AFRL/VSBX

11. SPONSOR/MONITOR'S REPORT NUMBER(S)**12. DISTRIBUTION / AVAILABILITY STATEMENT**

Approved for Public Release; Distribution Unlimited.

*AER, Inc., Lexington, MA

13. SUPPLEMENTARY NOTES

REPRINTED FROM PROCEEDINGS: 43RD AIAA AEROSPACE SCIENCES MEETING AND EXHIBIT
10-12 Jan 2005, RENO, NV

14. ABSTRACT

Geophysics research spacecraft are often covered partially with thin layers of dielectrics such as kapton or thermal blanket materials. Analytical modeling of the charging of a dielectric spacecraft in sunlight needs to go beyond the monopole potential and include a dipole term. If the capacitances of the dielectric layers are sufficiently large and the spacecraft spin rate is sufficiently fast the potentials may be determined on the basis of spin averaged spectra of electron and ion fluxes. In such a condition the potential distribution resembles that of a monopole-quadrupole system. We formulate the monopole-quadrupole case and compare it to the monopole-dipole model.

15. SUBJECT TERMS

Spacecraft charging Monopole-dipole model Monopole-quadrupole model
Spinning spacecraft Charging in sunlight

16. SECURITY CLASSIFICATION OF:**a. REPORT**

UNCLAS

UNCLAS

c. THIS PAGE

UNCLAS

17. LIMITATION OF ABSTRACT

SAR

18. NUMBER OF PAGES**19a. NAME OF RESPONSIBLE PERSON**

Shu T. Lai

19b. TELEPHONE NUMBER (include area code)

781-377-2932

Monopole-Quadrupole Model of Spacecraft Charging in Sunlight

Maurice Tautz[#]

AER, Inc., Lexington, MA 01730

and

Shu T. Lai^{**}

Space Vehicles Directorate, Air Force Research Laboratory, Hanscom AFB, MA 01731

Geophysics research spacecraft are often covered partially with thin layers of dielectrics such as kapton or thermal blanket materials. Analytical modeling of the charging of a dielectric spacecraft in sunlight needs to go beyond the monopole potential and include a dipole term. If the capacitances of the dielectric layers are sufficiently large and the spacecraft spin rate is sufficiently fast the potentials may be determined on the basis of spin averaged spectra of electron and ion fluxes. In such a condition the potential distribution resembles that of a monopole-quadrupole system. We formulate the monopole-quadrupole case and compare it to the monopole-dipole model.

Nomenclature

| | | |
|----------|---|---|
| A | = | quadrupole/dipole strength relative to the monopole |
| A_n | = | coefficients giving the strength relative to the monopole |
| K | = | monopole potential |
| P_n | = | n^{th} order Legendre polynomial |
| R_b | = | barrier radius |
| R_B | = | maximum barrier radius |
| V | = | potential outside spacecraft |
| V_B | = | maximum barrier height |
| V_N | = | surface potential at $t = 0^\circ$ |
| V_M | = | surface potential at $t = 90^\circ$ |
| V_S | = | surface potential at $t = 180^\circ$ |
| V_{SS} | = | sun to shade potential ratio |
| r | = | radius |
| t | = | polar angle |
| t_b | = | polar angle at the barrier |
| t_B | = | polar angle at the maximum barrier radius |
| t_W | = | angular width of barrier |

[#] Member of technical staff, AER, Inc., Lexington, MA.

^{**} Senior research physicist, Air Force Research Laboratory; Associate Fellow, AIAA.

20050412 006

I. Introduction

Daylight charging of a spherical object covered with dielectric was first studied by Mandell et.al.¹, Higgins² and Besse and Rubin³. The Laplacian potential distribution around the satellite is represented by a combination of monopole and dipole terms. Axial symmetry around the sun direction is assumed, so the object could be either stationary or rotating. The monopole and dipole terms combine to form a potential barrier outside the sunlit surface which acts to suppress the escape of photoelectrons, leading ultimately to current balance. In this paper we describe a similar model, where the dipole term is replaced by a quadrupole contribution. In the monopole-quadrupole system, the satellite spins about the polar axes of the sphere and the sun is interpreted to be shining on the belly-band. Axial symmetry around the spin pole is assumed and thus the satellite must be rotating rapidly so that only revolution time averaged photoemission is experienced. An axially symmetric potential barrier forms at the belly-band to block photoelectrons, enabling the net current to go to zero. The potentials give the first order charging response in daylight of a roughly spherical, non-conducting, fast spinning spacecraft in a low density space environment.

To facilitate comparison, the monopole-quadrupole and monopole-dipole analytic models are developed in parallel. There are two free parameters in the models. The first parameter, K , is the monopole potential. The second parameter, A , is the quadrupole/dipole strength relative to the monopole. The basic equations of the models and the parameters are described in section 2. In section 3, numerical solutions are outlined and results are given. Section 4 contains summary remarks.

II. The Monopole/dipole/quadrupole Expansion

The meaning of rapid spin is relative to satellite surface charging times. If the spin period is long compared to the differential charging time of dielectric surface elements, the surface is able to respond to the sun and the motion may be considered slow. If the spin period is short compared to the time it takes a dielectric surface to charge, the motion is considered to be fast. In this case the surface would respond only to spin averaged solar illumination.

Consider a dielectric-covered spherical satellite that is rotating rapidly in sunlight, so that only spin averaged effects are important. If the ambient space charge density is low, which can be the case at geosynchronous altitudes, the potentials outside the satellite would be given approximately by an axially symmetric solution to Laplace's equation. In spherical coordinates, the Laplacian potentials can be written in the form (see Schwartz⁴):

$$V(r, t) = \frac{K}{r} \sum_{n=0}^{\infty} \frac{A_n P_n(t)}{r^n} \quad (1)$$

where r is the radius and t is the polar angle. The sum is over $n = 0, 1, 2, \dots$ and $P_n(t)$ is the n^{th} order Legendre polynomial. The constant coefficient K is the monopole potential and the coefficients A_n give the strength relative to the monopole. If we keep the three lowest order terms, the potential will be

$$V(r, t) = \frac{K}{r} \left(1 + \frac{A_1 P_1(t)}{r} + \frac{A_2 P_2(t)}{r^2} \right) \quad (2)$$

where A_1 is the dipole strength and A_2 represents the quadrupole. If we assume a unit sphere, we have on the surface

$$V(1, t) = K (1 + A_1 P_1(t) + A_2 P_2(t)) \quad (3)$$

The monopole-dipole case corresponds to $A_1 = -A$, $A_2 = 0$ and the monopole-quadrupole case is specified by $A_1 = 0$, $A_2 = A$. We note that the minus sign in the monopole-dipole case is arbitrary and

agrees with previous treatments: a plus sign would put the sun at the opposite spin pole. The K and A parameters depend on the balance of the incoming and outgoing satellite surface currents and, since the ambient currents are here not assumed to be known, are free parameters of the models.

The overall shape of the potential distributions can be seen by looking at the north, middle and south surface potentials at the polar angles $t = 0, 90$ and 180 degrees respectively. These potentials are shown below, with the monopole-quadrupole system on the left and the monopole-dipole case on the right, enclosed in curly brackets

$$V(1,0) = V_N = K(1+A) \quad \{ K(1-A) \} \quad (4)$$

$$V(1,90) = V_M = K(1-A/2) \quad \{ K \} \quad (5)$$

$$V(1,180) = V_S = K(1+A) \quad \{ K(1+A) \} \quad (6)$$

In these equations, we normally have $K < 0$ for negative voltage charging and $A > 0$ for sunlit charging. The monopole-quadrupole system has equal potentials at the poles, and a lower (negative) potential at the belly-band. In contrast, for the monopole-dipole system, the potentials increase (negatively) in going from the north to south poles.

The lower limit on A is determined by the charging threshold, discussed in the next section. A practical upper limit on A can be taken as the point where the lowest potentials go to zero. This gives $A = 1$ for the monopole-dipole system and $A = 2$ for the monopole-quadrupole case.

III. Solution of the Models

Photoemission currents (positive) usually dominate ambient currents in the magnetosphere, yet negative charging is reported in daylight. A mechanism for sunlight charging is well known. The shaded surfaces charge up and the fields wrap around the object to the sunlit side. A potential barrier forms outside of the sunlit surface to trap escaping photoelectrons, allowing current balance. The models are based on this barrier dominated scenario. To obtain an analytic solution to the problem we neglect a self-consistent photosheath, which would require Poisson's equation and particle tracking.

For a potential barrier to form, we have the condition

$$dV(r,t)/dr = 0 \quad (7)$$

and using the previous expression (2) for $V(r,t)$, we get

$$\frac{K}{r^2} \left(1 - \frac{2A_1 P_1(t)}{r} + \frac{3A_2 P_2(t)}{r^2} \right) = 0 \quad (8)$$

Solving this equation for r gives the barrier radius $R_b(A,t)$. Here and below we give the result for the monopole-quadrupole system (the corresponding quantities for the monopole-dipole model are summarized in Table 1)

$$R_B(A,t) = (-3A_2 P_2)^{1/2} = \left(\frac{3}{2} A (1 - 3 \cos^2 t) \right)^{1/2} \quad (9)$$

A maximum barrier radius, R_B , occurs at some angle t_B . For the monopole-quadrupole model, R_B is a maximum when $-P_2$ is at a maximum, which occurs at $t_B = 90^\circ$ and we have $R_B = (3/2A)^{1/2}$. We can interpret the angle t_B as specifying the sun direction. A barrier forms outside the sphere for A -values above a threshold which can be determined using the condition $R_B = 1$, which gives $A = 2/3$.

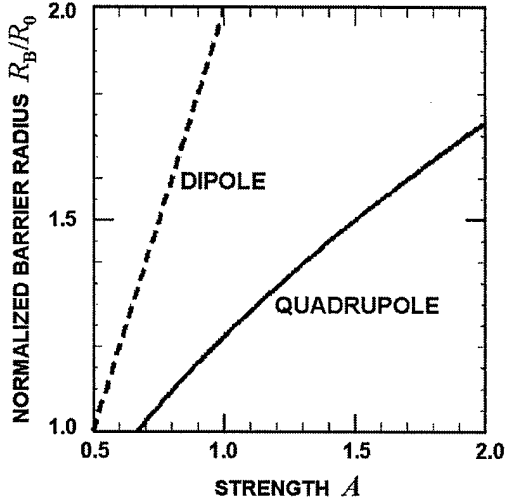


Figure 1. Maximum barrier radius as a function of strength A for the dipole and quadrupole models. The barrier radius increases monotonically with A from the threshold value of unity.

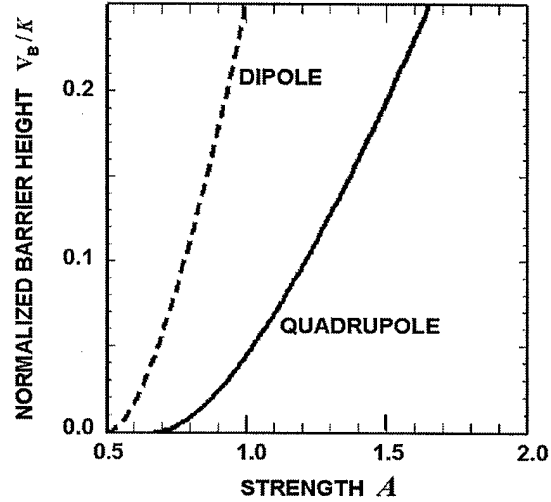


Figure 2. Maximum barrier height V_B (normalized by K) for the dipole and quadrupole models. The barrier heights monotonically increase from zero at the thresholds.

Figure 1 shows the maximum barrier radius for the two models in the range of interest. The barrier radius increases monotonically with A , from the threshold value of one. The maximum height of the potential barrier is given by

$$V_B = V(R_B, t_B) - V(1, t_B) \quad (10)$$

For the monopole-quadrupole case, we find a normalized barrier height

$$V_B = K \left(\left(\frac{2}{3} \right)^{3/2} A^{-1/2} + \frac{A}{2} - 1 \right) \quad (11)$$

A plot of V_B/K for the two models is given in Figure 2. The barriers monotonically increase from zero at the thresholds.

We can also determine the angular width, t_w , of the barrier region, given an A -value above threshold. The condition $R_B = 1$ gives the angle t_1 at which the barrier returns to the surface and hence $t_w = \pm (t_B - t_1)$. Solving for the monopole-quadrupole case, we get

$$t_1 = \cos^{-1} \left(\sqrt{\frac{A-2/3}{3A}} \right) \quad (12)$$

At threshold $t_w = 0$ and at maximum A we have $t_w = \pm 28.1^\circ$. Since the maximum barrier width is less than the nominal angular width of photoemission exposure $\pm 90^\circ$, we do not have self-consistent photoemission dynamics.

The sun to shade potential ratio, V_{ss} , in the monopole-quadrupole case is given by

$$V_{ss} = \frac{V_M}{V_S} = \frac{1 - A/2}{1 + A} \quad (13)$$

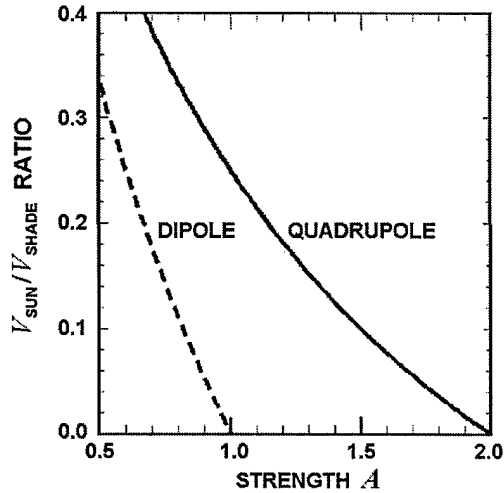


Figure 3. The sun to shade potential ratio as a function of strength A for the dipole and quadrupole models.

which at threshold is $2/5$. A comparison plot of V_{SS} is given in Figure 3. Since V_{SS} for both cases is monotonically decreasing, the models predict that this ratio will be below the threshold values.

Figure 4 shows the monopole-quadrupole potentials, normalized to K , in the physical space surrounding the sphere. The contour plot shows a $Y = 0$ slice of data expressed in X, Y, Z coordinates, which are normalized to the sphere radius. The A parameter has been selected so that the barrier potential ratio $V_B / K \sim 0.01$. This sets up a barrier of -10 V, given a monopole potential of -1000 V. An axially symmetric potential barrier forms at the belly-band. The contour plot for the corresponding monopole-dipole case is given in Figure 5.

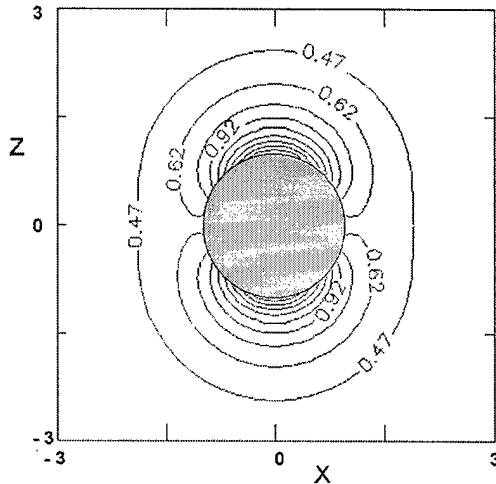


Figure 4. Potentials for the Monopole-Quadrupole system in the plane $Y=0$. The parameters used are $t_B = 90^\circ$, $A = 0.811$, $R_B = 1.103$, $V_B/K = 0.01$.

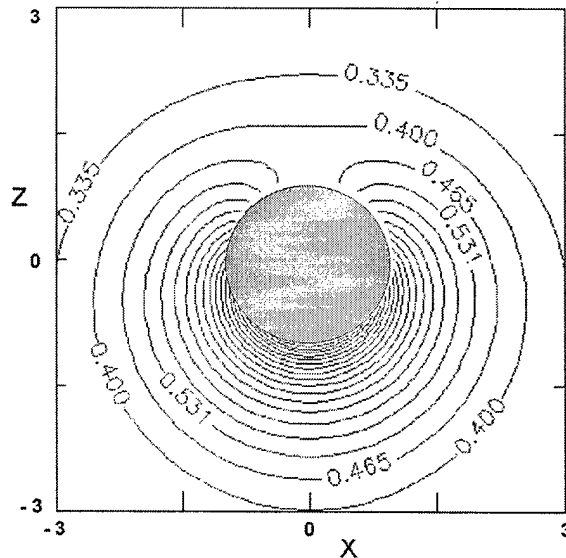


Figure 5. Potentials for the Monopole-Dipole system in the plane $Y=0$. The parameter used are $t_B = 0$, $A = 0.576$, $R_B = 1.152$, $V_B/K = 0.01$.

IV. Summary

For a spherical fast-spinning dielectric-covered satellite that is located in a low density ambient space plasma, we have developed a simple analytic model, the monopole-quadrupole, for charging in sunlight. The model sets up an axially symmetric potential barrier at the belly-band of the satellite which acts to suppress photoemission and leads to current balance. We can interpret the model as representing spacecraft charging with the sun at right angles to the spin axis. The belly-band charges less (negatively) than the spin poles and the sun to shade potential ratio lies below its threshold value.

The monopole-quadrupole and the monopole-dipole systems are similar in that they ignore many details of satellite construction and charging environment in order to capture the main effects.

For both, the analysis is based on axial symmetry and Laplacian potentials. The major differences between the models are: (1) The sun locations are 90 degrees apart (the belly-band versus the spin pole), (2) The charging thresholds are slightly different ($A=2/3$ versus $1/2$), (3) The sun to shade ratios are similar, but not the same ($V_{ss}=2/5$ versus $1/3$).

In the monopole-dipole system the dark side is constantly hidden from the sun during a spin revolution and this model includes the slow spin limit. For the monopole-quadrupole system the shaded side is instantaneously changing and the results are only valid for fast rotation rates, where spin averaged photoemission becomes a good approximation.

References

¹Mandell, M., I Katz, G. Schnuelle, P. Steen, and J. Roche, The decrease in effective photo-currents due to saddle points in electrostatic potentials near differentially charged spacecraft, *IEEE Trans. Nuc. Sci.*, Vol.26, No.6, Dec, 1978, p.1313-1317.

²Higgins, D., An analytic model of multi-dimensional spacecraft charging fields and potentials, *IEEE Trans. Nuc. Sci.*, Vol.26, No.6, Dec 1979, p.5162.

³Besse, A. and A. Rubin, A simple analysis of spacecraft charging involving blocked photoelectron currents, *J. Geophys. Res.*, Vol.85, No. A5, 1980, pp.2324-2328.

⁴Schwartz, M., *Principles of Electrodynamics*, McGraw-Hill, New York, 1972.

Table 1: Comparison of the Quadrupole verses Dipole Model

| | Monopole-Quadrupole Model | Monopole-Dipole Model |
|-----------------|--|---|
| $R_b(A, t)$ | $\left(\frac{3}{2} A (1 - 3 \cos^2 t)\right)^{1/2}$ | $2 A \cos t$ |
| t_B | 90° | 0° |
| $R_B(A, t_B)$ | $\left(\frac{3}{2} A\right)^{1/2}$ | $2A$ |
| V_B | $K \left(\left(\frac{2}{3}\right)^{3/2} A^{-1/2} + \frac{A}{2} - 1 \right)$ | $K \frac{(2A-1)^2}{4A}$ |
| t_1 | $\cos^{-1} \left(\sqrt{\frac{A-2/3}{3A}} \right)$ | $\cos^{-1} \left(\frac{1}{2A} \right)$ |
| V_{ss} | $\frac{V_M}{V_s} = \frac{1-A/2}{1+A}$ | $\frac{V_N}{V_s} = \frac{1-A}{1+A}$ |
| A (threshold) | $2/3$ | $1/2$ |
| A (upper) | 2 | 1 |